JOURNAL OF COMPUTATIONAL PHYSICS 118, 320–328 (1995)

Application of the Implicitly Updated Arnoldi Method with a Complex Shift-and-Invert Strategy in MHD

M. N. KOOPER

Institute for Plasma Physics, FOM Rijnhuizen, Nieuwegein, The Netherlands

H. A. VAN DER VORST

Department of Mathematics, Utrecht University, Utrecht, The Netherlands

AND

S. POEDTS AND J. P. GOEDBLOED*

Institute for Plasma Physics, FOM Rijnhuizen, Nieuwegein, The Netherlands

Received November 1, 1993

The implicitly updated Arnoldi method introduced by Sorensen with an internal QR-iteration is a very useful eigenvalue solver for nonsymmetric eigenvalue problems. To make this method rigorous in finding internal eigenvalues, a complex shift-and-invert strategy is used. Therefore a complex variant of the method has been constructed and the method has been compared with a Lanczos method, as implemented by Cullum *et al.*, for a practical problem in magnetohydrodynamics. © 1995 Academic Press, Inc.

1. INTRODUCTION

Magnetohydrodynamics (MHD) involves the study of the interaction of an ionized gas (a plasma) and a magnetic field. The MHD equations describe the macroscopic behaviour of a plasma in a magnetic field. These equations form a system of coupled nonlinear partial differential equations. A normal mode analysis of the linearized MHD equations leads to a complex eigenvalue problem. A finite element discretization in combination with the Galerkin method then yields an eigenvalue problem of the standard form

$$Ax = \lambda Bx, \tag{1}$$

with λ the (complex) eigenvalue, A a non-Hermitian matrix, and B a symmetric and positive definite matrix. Due to the use of finite elements for the spatial discretization, the matrices A and B have a tridiagonal block structure.

Many problems in physics and engineering require the discretization of partial differential equations and lead to a complex eigenvalue problem of the form (1). In quantum mechanics, e.g., the operators involved are Hermitian. These operators can always be diagonalized which led to the beautiful spectral theory. The MHD equivalent of this, however, requires the solution of nonsymmetric eigenvalue problems which is still by no means standard. Yet, MHD spectroscopy [6, 7] holds promises for the better understanding of magnetically confined plasmas. This is crucial for progress in controlled thermonuclear fusion research and for a deeper insight in the dynamic behavior of magnetic structures on the sun and other stars. In this paper we introduce a complex variant of the implicitly updated Arnoldi method [18] as a rigorous solver of this specific MHD eigenvalue problem. This method may be applied to any similar, generalized eigenvalue problem as this method is very accurate and competitive with any other eigenvalue solver.

In MHD problems the eigenvalues come in conjugate complex eigenpairs and refer to three types of modes: the fast magnetosonic modes, the Alfvén modes, and the slow magnetosonic modes. For the stability of magnetically confined plasmas one is mainly interested in the Alfvén spectrum. It has been shown [11] that the desired eigenvalues lie on curves in the complex plane (see Fig. 5). The eigenvalues which are of interest belong to the Alfvén branch. In the strongly magnetized plasmas that are studied in the laboratory in the context of controlled thermonuclear fusion research, as well as in the elongated magnetic loops observed on the solar corona, the eigenvalues of the Alfvén branch are small in magnitude compared with the extreme eigenvalues. The fast magnetosonic eigenvalues belonging to the fast magnetosonic subspectrum are very dominant and increase in magnitude as the discretization of the MHD equations is refined. The Alfvén part of the spectrum

* The authors thank Sander Beliën for his useful contributions to the optimization of the applied codes.

0021-9991/95 $6.00

is therefore dominated by unwanted eigenvalues in the fast magnetosonic spectrum, and for this reason the application of a (complex) shift and invert strategy is needed to make the desired part of the spectrum dominant. Using a shift σ in Eq. (1), we derive the new eigenvalue problem

$$\hat{A}x = \mu x, \qquad \text{with } \hat{A} = (A - \sigma B)^{-1}B \text{ and } \mu = \frac{1}{(\lambda - \sigma)}. \quad (2)$$

The choice of an optimal shift σ is surely not trivial. When σ is chosen complex, $\hat{A}$ becomes a matrix with complex elements and (2) becomes a complex eigenvalue problem; while choosing σ real we keep real arithmetic, which is an advantage in actual computing. This will be discussed more extensively in Section 3.

A popular algorithm for finding a few eigenvalues in large, symmetric eigenvalue problems is the Lanczos method [9]. This method has been extended for the nonsymmetric problem. Examples are the two-sided Lanczos method [3] and an orthogonal extension, the Arnoldi method [1]. The Lanczos method will be discussed briefly in Section 4. The Arnoldi method has the nice property that the appearance of spurious eigenvalues, when solving the generalized eigenvalue problem, may be avoided because of the complete orthogonalization of the Arnoldi vectors. However, high computational costs and a large demand for data storage have made the regular Arnoldi method rather unpopular. Alternatives for the nonsymmetric case, the k-step Arnoldi methods, have been proposed in various publications (e.g. in [16, 17, and 2]). Those methods have the advantage of low storage requirements. This is conceived by trying to approximate an invariant subspace of dimension k corresponding to k desired eigenvalues of $\hat{A}$ by restarting the Arnoldi factorization after k steps. However, important information is typically lost after a restart. This is partly solved in [13] where the Arnoldi factorization is restarted after $k + p$ steps with a vector composed of the k Ritz vectors, which approximate the desired, invariant subspace in some sense. The explicit computation of the Ritz vectors is very expensive, and it would be more advantageous to make a cheap update of the k-dimensional subspace, created by the Arnoldi factorization, every iteration step and iteratively force the residual to zero. Such an alternative approach for computing an invariant subspace of order k was proposed by Sorensen [18].

In this method one starts with k Arnoldi steps to create an initial approximation of the invariant subspace of dimension k corresponding to k desired eigenvalues. This subspace is repeatedly expanded with p vectors found through the Arnoldi iteration. On this $k + p$ dimensional subspace an implicitly shifted QR iteration with p implicit shifts (the unwanted Ritz values) is applied, which compresses the desired information into the first k vectors and drives the residual in the projected operator to zero. In Demmel *et al.* [4] it is noted explicitly that the computed k dimensional space after i times of this expansion and compression process will be a subset of the $k + i \times p$ dimensional subspace one would get without compression. One may expect that the intersection of the desired invariant subspace with this compressed subspace will be close to the intersection with the larger $k + i \times p$ dimensional subspace. Our experiments indicate this to be a successful approach for MHD problems as well.

In Section 2 we give a brief overview of the implicitly updated Arnoldi method (IUAM) in which we closely follow the presentation of [18]. For further details we refer the reader to this paper.

2. THE IMPLICITLY UPDATED ARNOLDI METHOD

The Arnoldi method is used to produce orthonormal vectors $v_1, v_2, \ldots$ such that after k steps the matrix $\hat{A}$ is projected into a $(k \times k)$ upper Hessenberg matrix H_k:

$$\hat{A}V_k = V_k H_k + r_k e_k^T = (V_k, v_{k+1}) \begin{pmatrix} H_k \\ \beta_k e_k^T \end{pmatrix}, \quad (3)$$

where r_k is the residual orthogonal to V_k; i.e.,

$$V_k^H r_k = 0,$$
$$\beta_k = \|r_k\|,$$
$$v_{k+1} = \frac{1}{\beta_k} r_k.$$

It is a well-known fact that $v_1, \ldots, v_k$ form an orthonormal basis for the Krylov subspace $\text{span}\{v_1, \hat{A}v_1, \ldots, \hat{A}^{k-1}v_1\}$ (see for example [5]). The Arnoldi method becomes increasingly expensive for growing k. Instead of a complete restart after k iterations an analogue of the implicitly shifted QR iteration is used.

The Krylov subspace is expanded by p Arnoldi steps, so that the projection of $\hat{A}$ is a $(k + p) \times (k + p)$ upper Hessenberg matrix H_{k+p}:

$$\hat{A}V_{k+p} = V_{k+p}H_{k+p} + r_{k+p}e_{k+p}^T = (V_{k+p}, v_{k+p+1}) \begin{pmatrix} H_{k+p} \\ \beta_{k+p}e_{k+p}^T \end{pmatrix}. \quad (4)$$

Let θ_j be a shift and let $(H_{k+p} - \theta_j I) = QR$ be an explicitly shifted QR-step, with Q orthonormal and R upper triangular. Then

$$(\hat{A} - \theta_j I)V_{k+p} - V_{k+p}(H_{k+p} - \theta_j I) = r_{k+p}e_{k+p}^T, \quad (5)$$

$$(\hat{A} - \theta_j I)V_{k+p} - V_{k+p}(QR) = r_{k+p}e_{k+p}^T, \quad (6)$$

$$(\hat{A} - \theta_j I)V_{k+p}Q - (V_{k+p}Q)(RQ) = r_{k+p}e_{k+p}^T Q, \quad (7)$$

$$\hat{A}(V_{k+p}Q) - (V_{k+p}Q)(RQ + \theta_j I) = r_{k+p}e_{k+p}^T Q. \quad (8)$$

With $\hat{H} = RQ + \theta_j I$, $\hat{H}$ is upper Hessenberg, and $\hat{V} = V_{k+p}Q$

is an orthonormal matrix. With an implicit shift strategy and combining (4) and (8) we find

$$\hat{A}V_{k+p}Q = (V_{k+p}Q, v_{k+p+1})\begin{pmatrix} Q^H H_{k+p} Q \\ \beta_{k+p} e_{k+p}^T Q \end{pmatrix}, \tag{9}$$

or, after applying p implicit shifts,

$$\hat{A}V^+ = (V^+, v_{k+p+1})\begin{pmatrix} H^+ \\ \beta_{k+p} e_{k+p}^T \hat{Q} \end{pmatrix}, \tag{10}$$

where $V^+ = V_{k+p}\hat{Q}$, $H^+ = \hat{Q}^H H_{k+p}\hat{Q}$, and $\hat{Q} = Q_1 Q_2 \cdots Q_p$. Q_j is the orthonormal matrix associated with the shift θ_j.

Note that:

- H^+ is the upper Hessenberg matrix after p QR-iterations on H_{k+p} [8].
- $\beta_{k+p} e_{k+p}^T \hat{Q} = (\underbrace{0, 0, \ldots, \tilde{\beta}}_{k}, \underbrace{b^T}_{p})$,

with $\tilde{\beta}$ as the kth coefficient.

With a partition of V^+ in a $(k \times k)$-block, and a $(p \times p)$-block, and H^+ in four blocks

$$V+ = (V_k^+, V_p^+),$$

$$H^+ = \begin{pmatrix} H_k^+ & M^+ \\ \hat{\beta} e_1 e_k^T & H_p^+ \end{pmatrix},$$

Eq. (10) can be reformulated as

$$\hat{A}(V_k^+, V_p^+) = (V_k^+, V_p^+, v_{k+p+1})\begin{pmatrix} H_k^+ & M^+ \\ \hat{\beta} e_1 e_k^T & H_p^+ \\ \tilde{\beta} e_k^T & b^T \end{pmatrix}. \tag{11}$$

Equating the first k columns on both sides of (11) gives

$$\hat{A}V_k^+ = V_k^+ H_k^+ + r^+ e_k^T, \tag{12}$$

so that

$$\hat{A}V_k^+ = (V_k^+, v^+)\begin{pmatrix} H_k^+ \\ \beta^+ e_k^T \end{pmatrix}, \tag{13}$$

where $v^+ = (1/\beta^+) r^+$, $r^+ \equiv (V_p^+ e_1 \hat{\beta} + v_{k+p+1}\tilde{\beta})$, and $\beta^+ = \|r^+\|$. Note that $(V_k^+)^H V_p^+ e_1 = 0$ and $(V_k^+)^H v_{k+p+1} = 0$. Thus (13) is a legitimate Arnoldi factorization of $\hat{A}$. Again a k-dimensional Krylov subspace $K_k(\hat{A}; v_1^+)$ is found, which can be expanded repeatedly by p additional Arnoldi steps, instead of restarting the Arnoldi iteration. With a suitable choice of the p shifts in QR the first k Arnoldi vectors are updated, so that $\beta^+ v^+ e_k^T$ is iteratively forced to zero in (13) and the k-dimensional subspace spanned by the columns of V_k^+ into the desired invariant subspace of $\hat{A}$. For the p shifts the unwanted Ritz values are used, which are found through a QR-iteration on H_{k+p}. Because $k + p \ll N$ this QR-iteration will be modest in storage requirements and computational costs. In the present paper the unwanted values are the Ritz values with smallest modulus.

The algorithm can be described as follows:

ALGORITHM 1: THE IMPLICITLY UPDATED ARNOLDI ALGORITHM.

(0) Select : v_1, k, p, tol;
(1) Initialize : $V_1 = v_1$; $H_1 = v_1^H \hat{A} v_1$; $r_1 = \hat{A}v_1 - v_1 H_1$;
(2) Start : do k Arnoldi steps to get V_k, H_k, r_k;
(3) While $\|r_k\| \geq$ tol do
  (1) Do p additional Arnoldi steps;
  (2) Calculate the Ritz values through $H_{k+p} =$ QR;
  (3) Select the p unwanted Ritz values as shifts;
  (4) Apply an implicit QR-iteration with p shifts to find V_{k+p}^+, H_{k+p}^+;
  (5) $V_k := V_{k+p}^+ \begin{pmatrix} I_k \\ 0 \end{pmatrix}$; $H_k := (I_k \quad 0)\, H_{k+p}^+ \begin{pmatrix} I_k \\ 0 \end{pmatrix}$;
  (6) $r := (v_{k+1}\hat{\beta}_k + r_{k+p}\sigma_{k+p})$; where $\sigma_{k+p} = e_{k+p}^T \hat{Q}_{k+p} e_k$;

Note that this method may converge very fast, because the residual is reduced every iteration step by applying p Arnoldi steps and p QR steps. Paige [10] has shown that the Lanczos iteration with a good initial vector forces $v^+ e_k^T \to 0$ in the symmetric case. Since after every update the new initial vector is better, one may expect that this process will converge even faster. Although there are counterexamples, similar observations have been made for the nonsymmetric case. In the Arnoldi process the quantity $|\beta^+|$ may not be expected to be small. However, the QR-iteration is known to have the property to force $|\beta^+| \to 0$ after every iteration step [8]. It is because of this "double" effect that this process may be so effective.

In the symmetric eigenvalue problem this combination of the Arnoldi method with an internal QR-iteration with p implicit shifts guarantees convergence [18]. In the nonsymmetric case the choice of real shifts may not be the optimal one. Usually the shifts are selected by a strategy based on the absolute value of the Ritz values. Although this occasionally may lead to poor convergence (Sorensen suggests other strategies) we have not encountered any difficulty with this strategy in our experiments.

3. APPLICATION OF A COMPLEX SHIFT AND INVERT STRATEGY

Iterative methods like Lanczos and Arnoldi usually converge to the dominant part of the eigenvalue spectrum, i.e., the extremal eigenvalues. In many physical systems one is interested in an internal part of the eigenvalue spectrum, such as the Alfvén

spectrum in MHD problems. To be able to find this part of the spectrum a transformed eigenvalue spectrum is needed in which the desired eigenvalues are enhanced to the dominant part of the spectrum. Applying a shift and invert strategy, as defined in (2), the new problem $\hat{A}x = \mu x$ has eigenvalues

$$\mu_i = \frac{1}{\lambda_i - \sigma},$$

with λ_i the solutions of (1). If the shift σ is chosen close to the desired eigenvalues, then these eigenvalues will appear in the transformed problem as eigenvalues with prominent magnitudes. With a good choice of σ these eigenvalues may be well separated from the other eigenvalues, and hence convergence will be fast. In the nonsymmetric eigenvalue problem (1) A and B are real, banded matrices, but the eigenvalues λ_i may come in complex conjugate pairs. To isolate a certain part of the eigenvalue spectrum a *complex* σ in (2) is necessary. In some cases a real shift is sufficient to locate certain eigenvalues, but in MHD this is typically not sufficient. Already in relatively small problems (i.e., $N = 416$) no convergence occurred. A complex shift is needed and therefore $\hat{A}$ in (2) is complex.

The major costs for computation and storage in the implicitly updated Arnoldi method come from the Arnoldi iteration: every iteration step $y = Bv_i$ is computed, $(A - \sigma B)v_{i+1} = y$ is solved by an LU-decomposition, and v_{i+1} is orthogonalized against $v_1, \ldots, v_i$. The internal QR-iteration takes only a small amount of time and storage. The costs of computation in complex arithmetic are nearly four times higher than in real arithmetic, and the storage requirements for complex numbers are twice the storage requirements for real numbers. Hence, keeping the computations in real arithmetic might be advantageous. To suppress computational costs, two goals can be formulated [12], which unfortunately can be in conflict:

1. stay in real arithmetic,
2. preserve any special structure of A and B, such as a band structure.

Goal 2 restricts our definition of $\hat{A}$, e.g. when B is invertible equation (1) can be reformulated as

$$(B^{-1}A - \sigma I)x = \mu x,$$

but with the implementation of $\hat{A} = (B^{-1}A - \sigma I)$ we loose the band structure in $\hat{A}$, and $\hat{A}$ becomes a dense matrix.

A trick can be used to stay in real arithmetic. The transformed eigenvalue problem (2) can be augmented to

$$\begin{pmatrix} A - \sigma_1 B & -\sigma_2 B \\ \sigma_2 B & A - \sigma_1 B \end{pmatrix}^{-1} \begin{pmatrix} B & 0 \\ 0 & B \end{pmatrix} y = \nu y, \qquad (14)$$

where $\sigma = \sigma_1 + i \cdot \sigma_2$. This new eigenvalue problem is of order $2N$, which increases the computational costs. The eigenvalues ν now come in pairs μ, as in Eq. (2), and $\overline{\mu}$. The eigenvectors y relate to the eigenvectors in (2):

$$y = \begin{pmatrix} I_N \\ i \cdot I_N \end{pmatrix} x \qquad \text{or} \qquad y = \begin{pmatrix} I_N \\ i \cdot I_N \end{pmatrix} \overline{x}.$$

With this suggestion the computations stay in real arithmetic, but the price may be high: The size of the problem is doubled, and the desired eigenvalues corresponding to the eigenvalues in Eq. (2) have to be identified. To find these true eigenvalues of the original problem,

$$\|A(I_N 0)y - \lambda B(I_N 0)y\|, \qquad \text{with } \lambda = \frac{1}{\nu} + \sigma,$$

needs to be checked to select the desired eigenvalues. This already implies a large amount of overhead, because all the eigenvectors are necessary while the actually desired eigenvectors could be obtained by a much cheaper inverse vector iteration. The introduction of conjugate eigenvalues $\overline{\mu}$ implies some other negative effects as well:

- slow convergence occurs because of the "clustering" of desired and conjugate eigenvalues around the shift σ (see Fig. 5);
- to identify the k desired eigenvalues at least $2 \cdot k$ eigenvalues in the real arithmetic problem (14) have to be determined;
- the bandwidth of $\hat{A}$ is increased by N.

For completeness we mention that Parlett and Saad [12] investigated the complex shift-and-invert strategy in real arithmetic. Their aim was to find eigenvectors through a subspace iteration, solving (2) but satisfying goals 1 and 2. They succeeded partly with a slightly different approach from ours: the banded structure was maintained, but a complex LU-decomposition to solve $(A - \sigma B)v_{i+1} = Bv_i$ was necessary. The other steps in the Arnoldi iteration could be continued in real arithmetic. However, they too could not avoid the introduction of conjugate eigenpairs through the augmentation of the original problem. The above considerations have led us to use a complex shift-and-invert strategy and to do our computations in complex arithmetic. Therefore a complex implementation of the IUAM has been constructed.

4. COMPARISON WITH A GENERALIZED LANCZOS METHOD

A frequently used method for large eigenvalue problems ($N > 1500$) in MHD is a generalized Lanczos solver, which was introduced by Cullum *et al.* [3]. This nonsymmetric, two-sided Lanczos method uses, like our approach, the complex shift-and-invert strategy and transforms $\hat{A}$ into a tridiagonal, complex, symmetric form T_n of order n. The eigenvalues of T_n, the Ritz values of $\hat{A}$, are approximations of the eigenvalues

of $\hat{A}$. In [3] several difficulties are discussed that may occur when solving nonsymmetric eigenvalue problems in general and the MHD problem in specific. Because most of those difficulties are similar to those for any eigenvalue solver we refer the reader to that article for details.

However, an important difference between the Lanczos method and the Arnoldi method is the orthogonalization of the Arnoldi vectors, which prevents spurious eigenvalues and the loss of accuracy because of a nonorthogonal transformation. A powerful property of the Lanczos method, on the other hand, is the low storage costs, because only six vectors need to be stored in total. In the Arnoldi method the storage of a vector per iteration is needed to be able to orthogonalize every new vector against the others. If $k + p \ll N$ is chosen, then the data storage will be modest for the complex IUAM. Because of this orthogonalization better approximations of the eigenvalues may be expected. If k is selected too large, then no convergence may occur, because it is possible that the k desired eigenvalues are not well separated from the unwanted part of the spectrum. Therefore the use of more than one complex shift σ_i in the shift-and-invert strategy may be necessary for large eigenvalue problems. Together with the user defined variables k and p, the method can be directed toward any relevant part of the spectrum of a generalized eigenvalue problem.

Several experiments with typical eigenvalue problems were executed in MHD. The single-fluid linearized MHD equations can be written in the following form in dimensionless units:

$$\frac{\partial \rho_1}{\partial t} = -\nabla \cdot (\rho_0 \mathbf{v}_1), \tag{15}$$

$$\rho_0 \frac{\partial \mathbf{v}_1}{\partial t} = -\nabla (\rho_1 T_0 + \rho_0 T_1) + (\nabla \times \mathbf{B}_0) \times \mathbf{B}_1 + (\nabla \times \mathbf{B}_1) \times \mathbf{B}_0, \tag{16}$$

$$\rho_0 \frac{\partial T_1}{\partial t} = -\rho_0 \mathbf{v}_1 \cdot \nabla T_0 - (\gamma - 1)\rho_0 T_0 \nabla \cdot \mathbf{v}_1, \tag{17}$$

$$\frac{\partial \mathbf{B}_1}{\partial t} = \nabla \times (\mathbf{v}_1 \times \mathbf{B}_0) - \nabla \times (\eta \nabla \times \mathbf{B}_1). \tag{18}$$

The resistivity, η, is assumed to be constant and the ratio of the specific heats, γ, is taken to be $\frac{5}{3}$. In these equations ρ, T, $\mathbf{B}$, and $\mathbf{v}$ are the plasma density, the temperature, the magnetic field, and the plasma velocity, respectively. The subscript 0 denotes an equilibrium quantity and subscript 1 denotes a Eulerian perturbation of the equilibrium quantity. Equations (15)–(18) are the continuity equation, the momentum equation for a nonviscous plasma, the equation for the variation of the internal energy, and the induction equation, respectively. The induction equation includes the Ohmic term due to the finite electric conductivity of the plasma. The resistive MHD equations have been linearized around a static equilibrium, i.e. $\mathbf{v}_0 = 0$ and $\partial/\partial t = 0$ when it operates on an equilibrium quantity. The divergence equation, $\nabla \cdot \mathbf{B}_1 = 0$, serves as an initial condition on $\mathbf{B}_1$: owing to Eq. (18), an initially divergence-free magnetic field will remain divergence-free. In the present paper a cylindrical plasma column is considered. In cylindrical coordinates r, θ, and z the linearized MHD equations (15)–(18) form a system of eight partial differential equations for eight unknowns, viz. ρ_1, v_{1r}, $v_{1\theta}$, v_{1z}, T_1, B_{1r}, $B_{1\theta}$, and B_{1z}, which is to be completed with appropriate boundary conditions.

The discretization of the system (15)–(18) is very similar to the discretization used in [3], but contains some differences. We will give the main steps of the discretization and stress the differences with the above-mentioned article. In the cylindrical plasma considered, the equilibrium quantities do not depend on θ and z. Therefore, the separation problem

$$f_1(r, \theta, z; t) = f_1(r; t) e^{im\theta + ikz} \tag{19}$$

is suitable for the perturbed quantities f_1. Here, the wave number m is an integer and the wave number $k = 2\pi n/L$ is quantized, with L the length of the cylinder. With the separation form (19) the system (15)–(18) reduces to a set of partial differential equations in r and t. In [3] an equivalent system is solved with variables $\mathbf{v}_1$, $\mathbf{p}_1$, and $\mathbf{B}_1$ (p_1 is the plasma pressure). In order to assure that the magnetic field is divergence-free, the θ-component of the magnetic field was eliminated by means of $\nabla \cdot \mathbf{B}_1 = 0$. This method has the disadvantage that it only applies to the case $m \neq 0$. In the present paper, therefore, the divergence-free condition on the magnetic field is satisfied in an alternative, more expensive, but more general way by expressing the magnetic field in terms of a vector potential $\mathbf{A}$:

$$\mathbf{B}_1 = \nabla \times \mathbf{A}. \tag{20}$$

In this alternative the system of ordinary differential equations describing the normal modes (with a time dependence proportional to $e^{-i\omega t}$) can be written in the form

$$(\mathbf{R} - i\omega \mathbf{S}) \cdot \mathbf{u} = 0, \tag{21}$$

where $\mathbf{u}$ is a state vector defined as

$$\mathbf{u}^T = (\hat{\rho}, v_1, v_2, v_3, \hat{T}, A_1, A_2, A_3), \tag{22}$$

with these variables defined as

$$\hat{\rho} = r\rho_1, \qquad \hat{T} = rT_1, \tag{23}$$

$$v_1 = rv_{1r}, \qquad A_1 = iA_r, \tag{24}$$

$$v_2 = i(B_{0z} v_{1\theta} - B_{0\theta} v_{1z}), \qquad A_2 = rA_\theta, \tag{25}$$

$$v_3 = irv_{1z}, \qquad A_3 = A_z. \tag{26}$$

The resistive MHD operator is represented by matrices $\mathbf{R}$ and $\mathbf{S}$ containing differential operators and equilibrium quantities. The system (15)–(18) is then discretized by means of a very

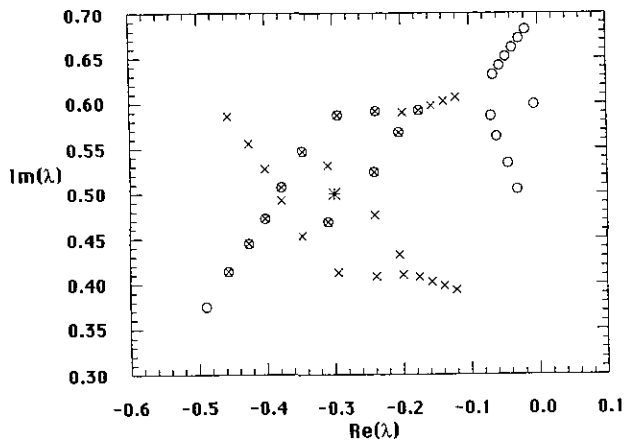

FIG. 1. Results of the Lanczos method (○) and the real IUAM (×) for $\eta = 10^{-4}$ and $N = 416$ (NG = 26) on a Cray-YMP.

accurate finite-element method, as discussed in [14]. Note that we now have eight equations for the eight unknowns defined above, whereas previously in [3] only six equations for the six unknowns v_{1r}, $v_{1\theta}$, v_{1z}, p_1, B_{1r}, and B_{1z} were exploited.

A finite-element discretization producing very accurate results by using a combination of cubic Hermite and quadratic finite elements is implemented. The components of the state vector **u** are approximated by a finite, linear combination of local expansion functions $h^k_{1,j}(r)$ and $h^k_{2,j}(r)$:

$$u^k(r) \approx \sum_{j=1}^{N} a^k_{1,j} h^k_{1,j}(r) + a^k_{2,j} h^k_{2,j}(r), \qquad k = 1, ..., 8, \tag{27}$$

with coefficients $a^k_{1,j}$ and $a^k_{2,j}$. Cubic Hermite finite elements are used for v_1, A_2, and A_3, and quadratic finite elements for $\hat{\rho}$, v_2, v_3, $\hat{T}$, and A_1. The introduction of two orthogonal shape functions per interval and per component of **u** raises the number of unknowns to 16NG, with NG the number of grid points. An application of the Galerkin method then leads to an eigenvalue problem of the form (1), where $\lambda = -i \cdot \omega$ denotes the eigenvalue and the matrices A and B are matrices in tridiagonal block form with blocks of size (16 × 16).

In our experiments we consider the modified eigenvalue problem (2) with A and B the matrices obtained from a test problem for a straight tokamak (periodic cylinder) surrounded by a vacuum and a perfectly conducting wall. The resistivity η is unequal to zero. The resistive MHD spectrum of a straight tokamak consists of discrete eigenvalues which lie on well-defined curves in the complex plane. These curves become independent of the plasma resistivity in the limit $\eta \to 0$. However, the number density of eigenvalues on these curves increases as η decreases. The Alfvén modes lie on a curve at the left side of the complex plane with a bifurcation point relatively close to the imaginary axis. The corresponding eigenfunctions are characterized by oscillatory behaviour. Hence, decreasing η requires an increase of the number of radial mesh points NG. Insufficient radial resolution, i.e., choosing NG too small, leads to spurious eigenvalues and incorrect Alfvén curves (see Experiment 1). In our experiments we varied both η and NG, the number of gridpoints. A smaller choice of η will imply a larger choice of NG, and the eigenvalue problem will become larger and will therefore be harder to solve. Bad convergence will occur around the bifurcation point when η is small, typically $\eta < 5 \times 10^{-5}$, due to the near dependency of the eigenfunctions around this point.

Experiments

The aim of the present paper is to show the rigor of the complex IUAM compared with the Lanczos method. It is found that the complex IUAM gives more accurate results than Lanczos. Moreover, with the new method more eigenvalues could be determined in less CPU time. Three experiments will be considered to support this statement. Experiment 1 (an MHD problem solved by the IUAM in real arithmetic) was mainly included to prove the necessity of complex arithmetic solving for the nonsymmetric eigenvalue problem. Experiments 2 and 3 are MHD problems of different order, which are solved by the Lanczos method and the complex IUAM. To make a fair comparison between these two methods we used the same convergence criterion, which was proposed by Paige [10], and the same shifts σ_i. The experiments were carried out on a Cray-YMP. To draw any conclusions on the accuracy of the methods the same MHD eigenvalue problems were solved on an IBM-3090 by a Lanczos method and refined by an inverse vector-iteration method. The IBM-3090 has a higher machine precision than the Cray-YMP. (A measure for the machine precision is ε, the smallest number on the computer for which $1 + \varepsilon \neq 1$. The IBM-3090 has an ε which is 30 times smaller than the ε on the Cray-YMP). The results found on the IBM-3090 are plotted in Figs. 1–5 (○).

Experiment 1. For $\eta = 10^{-4}$ an equidistant radial grid with

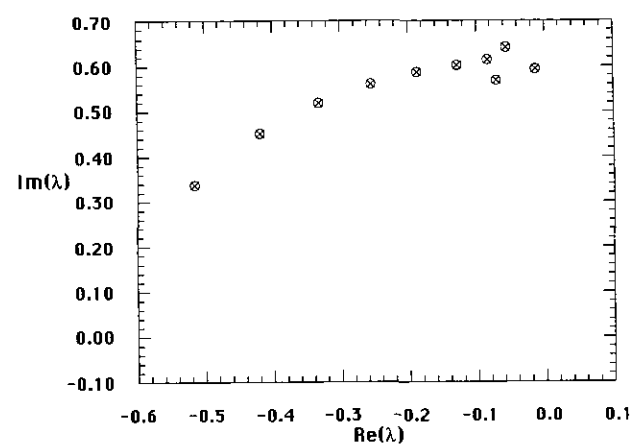

FIG. 2. The results of Lanczos on a Cray-YMP (×) and the "correct" Alfvén curve (○), for $\eta = 10^{-3}$ and $N = 1616$ ($N = 101$).

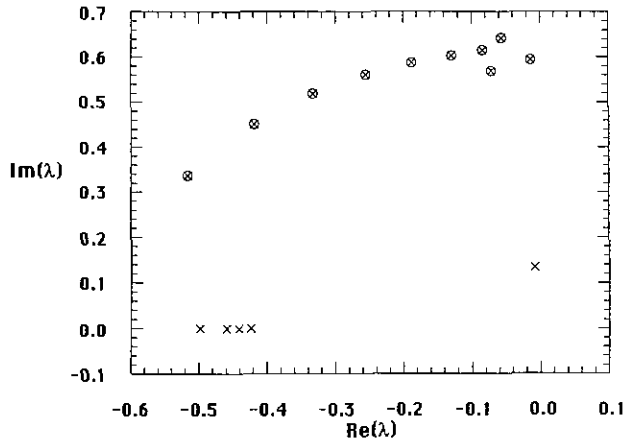

FIG. 3. The results of complex IUAM on a Cray-YMP (×) and the "correct" Alfvén curve (○), for $\eta = 10^{-3}$ and $N = 1616$ ($N = 101$).

26 gridpoints ($N = 416$) was used. We solved (14) by the IUAM in real arithmetic, using only one shift $\sigma = (-0.3, 0.5)$. In Fig. 5 approximations of the eigenvalues found by the real IUAM (×), and by the Lanczos method (○) were plotted. For the IUAM $k = p = 30$ was chosen, and for the Lanczos method we computed a tridiagonal matrix T_{50} of order 50 (for details see [3]). We note that the choice of NG = 26 for the given η led to spurious eigenvalues in the Alfvén branch of the spectrum (compare these results with Fig. 5 in which the Alfvén branch found by the complex IUAM is plotted for $\eta = 10^{-4}$ and NG = 201). Due to computer memory requirements of the IUAM in real arithmetic (the bandwidth of $\hat{A}$ in experiment 1 is 447), increasing NG would lead to very high storage costs. The IUAM converged in 3 iterations and yields 30 approximations of eigenvalues. However, only 15 approximations are approximations of the eigenvalues of the original problem (1). One may note the clustering of the desired and conjugate eigenvalues around σ (*). When no information about the location of the Alfvén branch is available it will be very hard to distinguish the desired and conjugate eigenvalues without any extra computations like the ones we mentioned in Section 3. The accuracy of the approximations of the desired eigenvalues is equal for both methods, but it took the IUAM over 10 sec of CPU time to converge, whereas the Lanczos method needed only 2.76 sec to find 23 eigenvalues of the Alfvén branch of the spectrum. In the other experiments we therefore used a complex version of the IUAM which has less restrictive computer memory requirements and leads to better results.

Experiment 2. For resistivity $\eta = 10^{-3}$ an equidistant radial grid with 101 gridpoints ($N = 1616$) is fine enough to give a physically correct Alfvén spectrum, i.e., the MHD eigenvalue problem is well defined and the Alfvén branch of the spectrum contains no spurious eigenvalues. We used three shifts, $\sigma_1 = (-0.01, 0.60)$, $\sigma_2 = (-0.25, 0.55)$, and $\sigma_3 = (-0.50, 0.20)$, to conceive the complete upper branch of the Alfvén curve solving (2) by both methods. In the Lanczos method a tridiagonal matrix of order 50 was repeatedly computed and in the complex IUAM $k = 10$ and $p = 20$ were chosen. In Fig. 5 the approximations of the eigenvalues found by the Lanczos method and the complex IUAM are plotted by ○, ×, respectively. For this relatively small MHD problem both methods converged quite well. The Lanczos method identified the upper part of the Alfvén branch in 12.3 sec Cray CPU time, and the complex IUAM needed 16.0 sec to find the upper part of the Alfvén branch, 1 eigenvalue on the imaginary axis, and 4 eigenvalues on the real axis. Pictorially, the results of both methods are equal to the approximations of the eigenvalues found on the IBM-3090 (○). Except for the three approximations of the eigenvalues around the bifurcation point, which were found by both methods with equal accuracy, the results of the complex IUAM were about 10 times more accurate than the approximations found by Lanczos.

In the high temperature tokamak plasmas studied in the con-

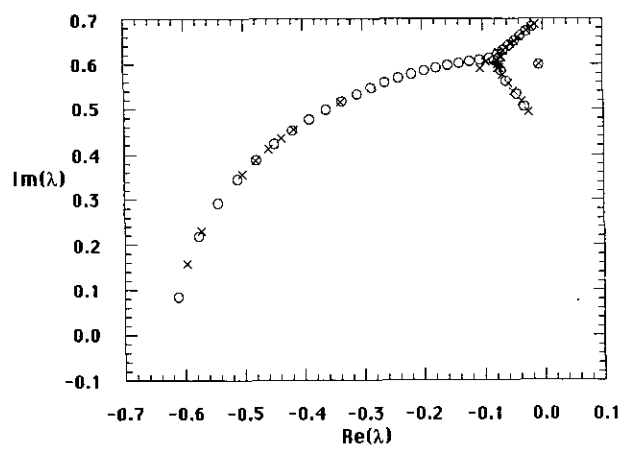

FIG. 4. The results of Lanczos on a Cray-YMP (×) and the "correct" Alfvén curve (○), for $\eta = 10^{-4}$ and $N = 3216$ ($N = 201$).

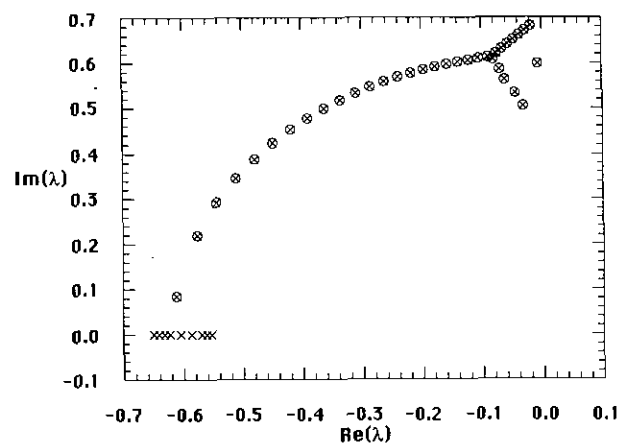

FIG. 5. The results of complex IUAM on a Cray-YMP (×) and the "correct" Alfvén curve (○), for $\eta = 10^{-4}$ and $N = 3216$ ($N = 201$).

text of controlled thermonuclear fusion research, the plasma resistivity is typically of the order 10^{-6} or smaller. Because of the poor convergence near the bifurcation point, the resistive spectrum cannot be completely computed for such well-conducting plasmas. Of course, one should try to choose η as small as possible in numerical simulations. In Experiment 3 the same test case with a smaller resistivity η is considered.

Experiment 3. Consider now a plasma with $\eta = 10^{-4}$. For this "low" plasma resistivity a grid with 201 gridpoints was necessary ($N = 3216$) to obtain a converged spectrum. Again this MHD problem was solved by both methods on a Cray-YMP. Four shifts were considered, $\sigma_1 = (-0.01, 0.60)$, $\sigma_2 = (-0.25, 0.65)$, $\sigma_3 = (-0.50, 0.50)$, and $\sigma_4 = (-0.60, 0.08)$. In the Lanczos method a tridiagonal matrix of order 50 was repeatedly calculated, and in the complex IUAM k and p were taken as 15. The results of both methods are plotted in Figs. 4 and 5. There is a clear difference between the accuracy in the approximations of the eigenvalues found by the Lanczos method and the approximations found by the complex IUAM. Comparing these results with the approximations of the eigenvalues found on the IBM (○), we note that scattering and the introduction of spurious eigenvalues occur in the approximations found by the Lanczos method in Fig. 4. The complex IUAM discovered 45 good approximations of the eigenvalues in 26.7 seconds Cray CPU-time, while Lanczos needed 31.8 seconds to find 25 poorly converged approximations for the eigenvalues.

5. CONCLUDING REMARKS

To identify specific parts of the eigenvalue spectrum for a generalized eigenvalue problem

$$Ax = \lambda Bx,$$

with A a nonsymmetric matrix with real elements and B a symmetric, positive definite matrix with real elements, we have considered a complex shift-and-invert strategy. This leads to a modified eigenvalue problem

$$\hat{A}x = \mu x,$$

with $\hat{A} = (A - \sigma B)^{-1}B$ a complex nonsymmetric matrix, $\mu = 1/(\lambda - \sigma)$, and σ the used shift. Although computing in complex arithmetic is more expensive in storage requirements and computational costs than it is in real arithmetic, it is shown that it may still be advantageous to work with this complex modified eigenvalue problem. The complex shift-and-invert strategy may be applied to the IUAM, which leads to a very accurate eigenvalue solver for the MHD eigenvalue problem. Because of its orthogonality properties, its relatively low storage requirements, and its avoidance of spurious eigenvalues, this method can compete with any other eigenvalue solver, such as the generalized Lanczos method and the k-step Arnoldi methods. Comparison with a generalized Lanczos method showed a convincing rigor of the complex IUAM.

Our derivations may be extended to more general eigenvalue problems, but the extension of the IUAM to complex arithmetic was done in the framework of MHD-spectroscopy [6, 7]. The aim of MHD spectroscopy is a better understanding of the structure and the dynamics of magnetically confined plasmas. For this purpose, numerically obtained MHD spectra and computer simulations of the plasma response to external excitation with an antenna system are compared with experimental observations of e.g. the dependence of the antenna impedance on the frequency in a tokamak device.

Clearly, such a comparison only makes sense when the numerical simulations are based on realistic theoretical models which take, among other things, the geometry of the configuration into account. Therefore, the straight tokamak considered in the present paper is not very well suited for the purpose of MHD spectroscopy. However, the aim of the present paper was to announce and explain the complex IUAM, and the straight tokamak Alfvén spectra were calculated in order to test and demonstrate this new eigenvalue solver. As the results are very promising, we will next tackle the real problem of MHD spectroscopy, viz. the determination of the MHD spectrum of axisymmetric toroidal plasmas with strongly noncircular cross sections. In such a geometry, strong poloidal mode coupling occurs which has a substantial influence on the MHD spectrum. However, as a result of the poloidal mode coupling one has to deal with large matrices which are typically an order of magnitude larger than the matrices obtained for cylindrical plasmas and used for testing the new eigenvalue solver in the present paper.

This is precisely why a complex implementation of the implicitly updated Arnoldi solver was developed. As a matter of fact, the matrices of the discretized problem become so large that the QR-method cannot be used because of too large computer memory requirements. In addition, the Lanczos solver does not yield satisfactory results for such large problems. However, the complex implementation of the implicitly updated Arnoldi method presented and discussed in this paper may be a good alternative for this problem and enable the determination of MHD spectra for realistic tokamak plasmas.

REFERENCES

1. W. E. Arnoldi, *Quart. Appl. Math.* **9,** 17 (1951).
2. F. Chatelin and D. Ho, *Math. Modelling and Numer. Anal.* **24,** 53 (1990).
3. J. Cullum, W. Kerner, and R. Willoughby, *Computer Phys. Comm.* **53,** 19 (1989).
4. J. W. Demmel, M. T. Heath, and H. A. van der Vorst, Parallel numerical linear algebra, in *Acta Numerica,* Vol. 2 (Cambridge Press, New York, 1993).
5. R. W. Freund, G. H. Golub, and N. M. Nachtigal, Iterative solution of

linear systems, in *Acta Numerica*, Vol. 1 (Cambridge Press, New York, 1992).

6. J. P. Goedbloed, MHD waves in the thermonuclear and solar plasmas, in *Trends in Physics, Prague, III, 1991*, edited by J. Kaczér, p. 827.
7. J. P. Goedbloed, G. T. A. Huysmans, S. Poedts, G. Halberstadt, W. Kerner, and E. Schwartz, Computation of resistive MHD modes in thermonuclear and astrophysical plasmas, in *Proc. IAEA Technical Committee Meeting on Advances in Simulation and Modelling of Thermonuclear Plasmas, Montréal, 1992*, edited by V. Demchenko and M. Shoucri, p. 316.
8. G. H. Golub and C. F. van Loan, *Matrix Computations*, 1st ed. (The John Hopkins Univ. Press, Baltimore, 1983).
9. C. Lanczos, An iteration method for the solution of the eigenvalue problem of linear differential and integral operators, *J. Res. Natl. Bureau Standards* **45**, 255 (1950).
10. C. C. Paige, Ph.D. thesis (University of London, 1971).
11. Y. Pao and W. Kerner, Analytic theory of stable resistive magnetohydrodynamic modes, *Phys. Fluids* **28**(1), 287 (1985).
12. B. N. Parlett and Y. Saad, *Linear Algebra Appl.* **88/89,** 575 (1987).
13. S. G. Petiton, *Appl. Numer. Math.* **10,** 19 (1992).
14. S. Poedts, A. J. C. Beliën, and J. P. Goedbloed, On the quality of resonant absorption as a coronal loop heating mechanism, *Solar Phys.* **151,** 271 (1994).
15. S. Poedts, M. Goossens, and W. Kerner, Numerical simulations of coronal heating by resonant absorption of Alfvén waves, *Solar Phys.* **123,** 83 (1989).
16. Y. Saad, Tchebychev acceleration techniques for solving nonsymmetric eigenvalue problems, *Math. Comput.* **42,** 567 (1984).
17. Y. Saad, Projection methods for solving large, sparse eigenvalue problems, in *Matrix Pencil Proceedings*, edited by B. Kagstrom *et al.* (Springer-Verlag, Berlin, 1982), p. 121.
18. D. C. Sorensen, *SIAM J. Mater. Anal. Appl.* **13**(1), 357 (1992).